SLAC-PUB-2549
AATF/80/24
June 1980
(T/E/A)

THE SLAC LINEAR COLLIDER*)

B. Richter
R. A. Bell, K. L. Brown, A. W. Chao, J. Clendenin, K. F. Crook, W. Davies-White, H. DeStaebler, S. Ecklund, G. E. Fischer, R. A. Gould, R. Helm, R. Hollebeek, M.-J. Lee, A. V. Lisin, G. A. Loew, R. E. Melen, R. H. Miller, D. M. Ritson, D. J. Sherden, C. Sinclair, J. Spencer, R. Stiening, H. Wiedemann, P. B. Wilson, C. Y. Yao

Stanford Linear Accelerator Center, Stanford University, Stanford, CA 94305

ABSTRACT

The SLAC LINEAR COLLIDER is designed to achieve an energy of 100 GeV in the electron-positron center-of-mass system by accelerating intense bunches of particles in the SLAC linac and transporting the electron and positron bunches in a special magnet system to a point where they are focused to a radius of about 2 microns and made to collide head on. We discuss the rationale for this new type of colliding beam system, describe the project, discuss some of the novel accelerator physics issues involved, and briefly describe some of the critical technical components.

1. INTRODUCTION

The progress of particle physics has always been intimately connected with the progress of accelerator technology. The past decade has seen the coming to maturity of the electron-positron colliding-beam storage-ring technique, and the machines built to exploit this technique have yielded most of what we have learned about the properties of new quarks, mesons, leptons, jets, etc. The physics arguments for continuing to higher energy in electron-positron colliding beams are compelling. However, the storage rings are becoming ever more costly. While it is clear that higher energies in electron-positron storage rings are technically possible, it is not clear that they are fiscally feasible.

The SLAC Linear Collider (SLC) discussed here has two main goals. One is to serve as the pioneer machine in a new technique to achieve high-energy electron-positron collisions at lower cost per GeV than the storage-ring technique used until now. The other is to increase the center-of-mass energy available in the electron-positron system to one above that required to investigate the unification of the weak and electromagnetic interactions which we now expect to become manifest at approximately 90 GeV in the center of mass.

The Collider is a variant of a new class of accelerators called Linear Colliders.[1] The true Linear Collider would use two linear accelerators aimed at each other to accelerate one intense bunch of electrons and one intense bunch of positrons each linac cycle. The beams would be focused to micron sizes and would collide between the two linacs. The particles would

*) Work supported by the Department of Energy, Contract DE-AC03-76SF00515.

(Invited talk to be presented at the XIth International Conference on High Energy Accelerators, CERN, Geneva, Switzerland, July 7-11, 1980.)

then be disposed of and not used again. These Linear Colliders could tolerate extremely high current densities at the collision point compared to those tolerable in storage rings. Further, because these machines do not store particles in a ring of magnets as do the storage rings, they do not require large amounts of rf power to make up for the synchrotron radiation energy losses that occur in storage rings. These two factors combine to give different scaling laws of size and cost vs energy for the two types of machines, and it is these different scaling laws which promise lower cost per unit energy for very high energy Linear Colliders compared to storage rings.

The cost of storage rings scales roughly as the square of the center-of-mass energy.[2] This scaling law arises because the rapid increase in RF voltage necessary to make up for synchrotron-radiation losses in the circular ring of magnets forces the storage-ring designer, in order to minimize the total cost of the project, to choose a radius and, hence, a cost for the machine which increases roughly as the square of the energy.

In contrast to storage rings, the true Linear Collider would not have to cope with synchrotron radiation. Hence, the length and the cost of an accelerator required to drive a linear colliding-beam system scale as the first power of the energy. Thus, at some energy a first-power scaling law will result in a less costly device than a quadratic scaling law.

The SLC does have a ring of magnets to guide the linac bunches to the collision point. At energies below roughly 70 GeV per beam, the synchrotron radiation emitted in these magnets has negligible effect on the total power required to operate the facility, while allowing the facility to be based on a single linac rather than on two linacs.

2. GENERAL DESCRIPTION OF THE PROJECT

The SLC is designed to operate at energies up to 100 GeV in the center-of-mass system. It can be increased in energy at a later time to 140 GeV in the center of mass should that become desirable. The main components of the project are the SLED II conversion of the SLAC Linac[3]; a transport system from the end of the linac to a small-aperture magnet ring; the magnet ring itself; a special focusing system near the interaction point; the necessary housing for the ring; an experimental hall and staging area; a high-power positron-production target; a positron booster; a transport system from the positron target at the two-thirds point of the linac back to the injection end of the linac; a new high-peak-current electron gun; two small storage rings to reduce the emittances of the electron and positron beams by radiation damping; pulse compressors to reduce the length of the bunches in the storage ring before injection into the linac; and the necessary instrumentation and control systems for both the linac and the Collider system. A schematic of the complete system is shown in Fig. 1, and Table 1 summarizes the important parameters.

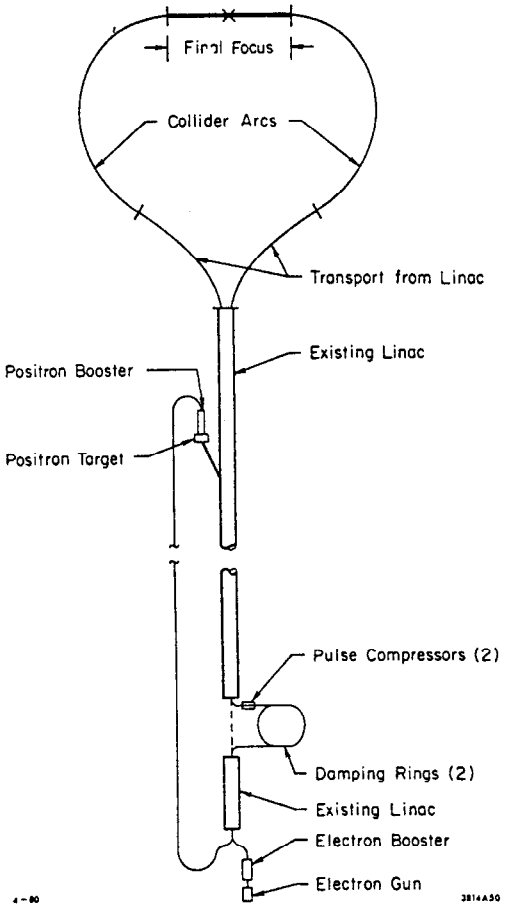

Fig. 1--General layout of the single pass collider.

Table 1

Parameters of the single pass collider at 50 GeV

A.	Interaction Point	
	Initial luminosity	$10^{30}cm^{-2}sec^{-1}$
	Invariant emmittance ($\sigma_x\sigma'_x\gamma$)	3×10^{-5} rad-m
	Repetition rate	180 Hz
	Beam size ($\sigma_x = \sigma_y$)	2 microns
	Equivalent beta function	1 cm
B.	Collider Arcs	
	Average radius	300 m
	Focusing structure	AG
	Cell length	5 m
	Betatron phase shift per cell	110°
	Full magnet aperture (x;y)	10;8 mm
	Vacuum requirement	$<10^{-2}$ Torr
C.	Linac	
	Accelerating gradient	17 MeV/m
	Focusing system phase shift	360° per 100 m
	Number of particles/bunch	5×10^{10}
	Final energy spread	±1/2%
	Bunch length (σ_z)	1 mm
D.	Damping Rings	
	Energy	1.21 GeV
	Number of bunches	2
	Damping time (transverse)	2.9 ms
	Betatron tune (x;y)	7.1; 3.1
	Circumference	34 m
	Aperture (x;y)	±5; ±6 mm
	Bend field	19.7 kg

A typical operation cycle of the collider goes as follows: The electron and positron damping rings each contain two bunches of 5×10^{10} particles at an energy of about 1.2 GeV. One of the positron bunches is extracted from the damping ring, passes through a pulse compressor which reduces the bunch length from the centimeter typical of the storage ring to the millimeter required for the linac, and is then injected into the linac. Both electron bunches are extracted from the electron damping ring, pass through an independent pulse compressor, and are injected into the linac behind the positron bunch. The typical spacing between bunches is 15 meters in the linac.

The three bunches are then accelerated down the linac. At the two-thirds point, the trailing electron bunch is extracted from the linac with a pulsed magnet and is directed onto a positron-production target. The positron bunch and the leading electron bunch continues to the end of the linac, where they reach an energy of 50 GeV.

At the end of the linac, the two opposite-charge bunches are separated by a DC magnet, pass through a transport system that matches the focusing of the linac to that of the main Collider ring, and then begin to travel around the ring in opposite directions. The Collider ring is composed of small-aperture magnets with very strong alternating-gradient focusing, which is required to hold down emittance growth in the Collider arcs. After emerging from the arcs, the bunches pass through an achromatic matching and focusing section which focuses the beams to a very small size at the collision point. Beyond the collision point, the bunches are extracted from the transport line by a pulsed magnet and brought to a beam dump.

The positrons produced by the electron bunch that was extracted at the two-thirds point of the linac pass through a focusing system at the positron source, a 200 MeV linear accelerator booster, a 180° bend, and an evacuated transport pipe located in the existing linac tunnel. This brings the positron bunch back to the beginning of the linac. At this point, the positron bunch passes through another 180° bend and is boosted to an energy of 1.2 GeV in the first sector of the existing linac and is then injected into the damping ring.

Because the emittance of the positron beam is very much larger than that required for Collider operation, a positron bunch must remain in the damping ring for approximately four radiation damping times, which corresponds to twice the time interval between linac pulses. Thus the positron bunch to be used in the next linac cycle is the one that is still stored in the damping ring from the previous cycle.

Electrons for Collider operation are produced from a special gun equipped with a subharmonic buncher and located at the beginning of the linac. Two bunches of electrons are produced, are boosted to 200 MeV in a dedicated section of linac, and are then injected into the same section of linac used to boost the positron bunch to 1.2 GeV. At the end of this section the 1.2 GeV electrons are injected into their own damping ring. The electron bunches at the time of injection into their damping ring have an emittance somewhat larger than required for Collider operation but considerably smaller than the emittance of the positron bunch and thus need only be damped for two damping times or one interpulse period. The entire cycle repeats 180 times per second.

The SLC is estimated to cost $63 million (March 1980 prices) and to require a construction period of three years.

3. BEAM DYNAMICS

3.1 General

It is straightforward to produce electron and positron bunches in the damping rings of the Collider with the required low emittance. When these bunches are transferred to the linac for acceleration to high energy and transport to the collision point, there are three important effects which will determine the final emittance of the bunch and, hence, the luminosity of the machine. First, there are both transverse and longitudinal space charge effects in the linac which tend to increase the transverse emittance and the energy spread of the bunch. The control of the transverse wake field effect sets the tolerances on beam alignment in the linac and on the stability of injection into the linac.

The second effect is caused by quantum fluctuations in the synchrotron radiation emitted in the bending magnets required to transport the electron and positron bunches from the linac to the collision point. Control of this effect determines the magnetic focusing lattice of the Collider arcs and sets tolerances on the allowed orbit distortions in these arcs.

The third effect is that of the beam-beam interaction. The megagauss fields in the very small radius bunches at the collision point profoundly affect the motion of the particles in the bunches as they pass through each other and, as we shall see later, can increase the effective luminosity in e^+e^- collisions.

3.2 Space Charge Effects

The space charge effects important here are of the head-to-tail type common in particle accelerators. The leading particles at the head of the bunch leave behind fields in the linac rf structure that act on particles which follow behind them in the bunch. Once the distribution of fields that a single particle leaves behind is known, it is straightforward to compute the space-charge effects on the ensemble of particles that constitute the bunch.

Two types of wake field trail behind a particle passing through the linac rf structure. There is a longitudinal wake which decelerates particles and a transverse wake which deflects particles. The longitudinal wake depends only on the distance between the particle generating the wake field and the particle upon which the wake field acts. The transverse wake is more complicated, for it not only depends on the distance separating the particles but is also proportional to the distance between the generating particle and geometrical center line of the linac. The modes which are important give effects independent of the transverse position of the following particles on which they act.

For bunch lengths appropriate to the Collider, the transverse wake increases with increasing separation between the particles while the

longitudinal wake decreases with increasing separation. Thus, the energy spread increases when the bunch is made shorter while the transverse emittance growth decreases. The bunch length which is a controllable parameter must be chosen to best balance these two space charge effects.

The effect of the longitudinal wake is shown in Fig. 2 which shows the current in the bunch and the total energy loss as a function of position caused by the longitudinal wake. The uncompensated effect of the wake is to introduce a ±2% energy spread over the length of the bunch -- far too much for the acromatic focusing system designed to produce the 2 micron radius spot at the interaction point.

The effect of the longitudinal wake on the energy spread can be compensated by accelerating the bunch off the crest of the accelerating field of the linac. Figure 3 shows the energy distribution of the bunch when accelerating 15 degrees ahead of the crest of the rf wave in the linac. Also shown in Fig. 3 is the energy spread of a low intensity bunch of the same shape accelerated at the same phase. The charge per bunch is required to be stable to about 10% to meet the required energy spread tolerances.

The transverse wake field is such that an intense bunch of particles traveling off-axis through a structure whose transverse dimensions are large compared to the length of the bunch will have all particles behind the head of the bunch deflected further away from the axis of the structure. Since the strength of the transverse wake increases with increasing distance, the back of the bunch will be pushed further from the axis than the front of the bunch and thus the projected area in transverse

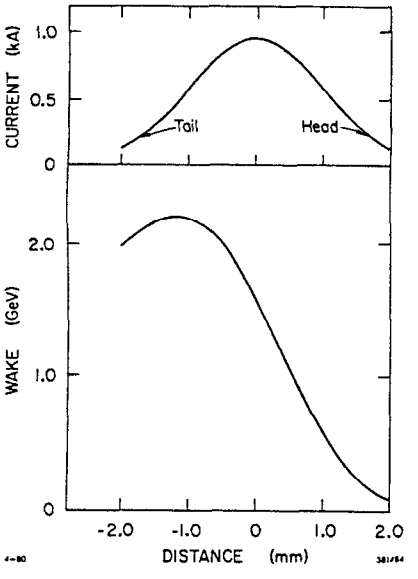

Fig. 2--The longitudinal wake for the design intensity of 5×10^{10} particles/bunch and the design bunch shapes, a Gaussian with $\delta = 1.0$ mm. The current in the bunch is 950 amperes.

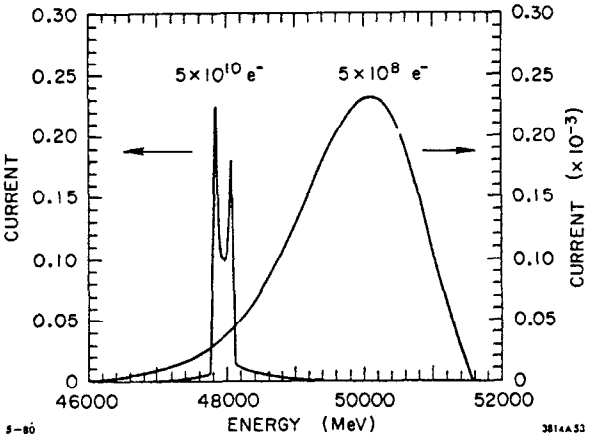

Fig. 3--Energy spread in the bunch with off-crest acceleration for two different bunch charges.

phase space occupied by all the particles of the bunch will effectively increase. In another contribution to this conference[4] the transverse wake field effects are discussed in detail. We will give the results as they apply to the Collider.

The control of the transverse wake-field effect requires that the particles in the bunch be held close to the axis of the accelerator. Emittance growth occurs both from injection errors which generate a coherent oscillation of the bunch around the axis of a perfectly aligned accelerator and from random misalignments of the accelerator structure. To some extent the effects of misalignment can be compensated for by a proper adjustment of the injection position and angle to cancel the effect of the misalignment-generated wake field. What we really require is a well aligned accelerator and good stability of injection into the linac.

As an example of the effect of injection errors, Table 2 shows that the stability required of the damping ring extraction kickers is a function of the number of particles in the bunch. Since the transverse wake field effect is exponential in the number of particles in the bunch, the tolerance is a strong function of this number. Figure 5 shows the effect of linac misalignments. Here we plot the average over the bunch of the reciprocal of the emittance as a function of the RMS misalignment tolerance. The required tolerance is about 100 microns. In practice with a relatively simple orbit correction scheme, the linac need only be aligned to about half a millimeter -- a simple task with the SLAC laser alignment system which is routinely used to an accuracy of a quarter of a millimeter.

3.3 Quantum Fluctuations

As the particles travel along the Collider arcs they lose energy in the form of synchrotron radiation. Quantum fluctuations in the synchrotron radiation lead to an increase of the beam emittance which is undesirable for good luminosity.

Table 2

Tolerance on injection stability into the linac set by the transverse wake effect. The first column gives the number of particles per bunch (N), and the second column gives the required fractional stability of the damping ring extraction kicker

N	Stability
5×10^{10}	1/2000
4×10^{10}	1/800
3×10^{10}	1/400

The emittance change is given by[5]

$$\frac{d\varepsilon}{ds} = \frac{\langle N\langle u^2\rangle H\rangle_s}{2cE_o^2} \qquad (1)$$

where the emittance is defined as the area of the phase space divided by π. Since we assume a Gaussian beam, we define the emittance for a standard deviation $\varepsilon = \sigma^2/\beta$. N is the number of photons emitted per second, $\langle u^2\rangle$ is the average photon energy squared, c is the speed of light, E_o is the beam energy, and H is a lattice function defined as

$$H = 1/\beta \left[\eta^2 + (\beta\eta' - \tfrac{1}{2}\beta'\eta)\right]^2 \qquad (2)$$

Here β is the horizontal betatron function, and η is the horizontal dispersion function. The average is taken along the beam line, and $N\langle u^2\rangle$ is

$$N\langle u^2\rangle = \frac{55}{24\sqrt{3}}\, r_e\, hmc^4\, \frac{\gamma^7}{\rho^3} \qquad (3)$$

If the total length is $\Delta s = \phi\rho$, with ϕ the total deflection in one arc, then from Eq. (1) we now get

$$\Delta\varepsilon \text{ (rad m)} = 2.1 \times 10^{-11}\, \phi E^5 \text{ (GeV}^5\text{)}\, \rho\, \langle H/\rho^3\rangle_s \qquad (4)$$

In order to minimize the emittance growth we have to choose a lattice that minimizes $\rho\langle H/\rho^3\rangle$. Obviously this demands the maximum possible bending radius ρ. The quantity H depends strongly on the parameters chosen for the lattice. For a simple FODO cell this quantity reaches a minimum[6] for a phase advance per cell of $\psi^\circ = 140^\circ$.

Calculations show that it is impossible to provide the necessary focusing for small emittance growth in a separated-function lattice design. We have decided, therefore, to use a combined-function lattice design. Since the beam travels through this lattice only once, we do not have to worry about the antidamping that is inherent in such a lattice.

For a phase advance per cell of about 110° (chosen to be a safe distance from the lattice stop band at 180° per cell), a cell length of 5.2 m, and a total bend angle of 211°, the emittance blowup is then

$$\Delta\varepsilon = 0.97 \times 10^{-10} \text{ rad m (at 50 GeV)} \quad . \qquad (5)$$

The emission of synchrotron radiation also increases the energy spread of the beam. For our lattice we obtain,

$$\Delta(\sigma_\varepsilon/E) = 1.6 \times 10^{-5} \text{ (at 50 GeV)} \ , \qquad (6)$$

which is much smaller than the ±0.5% energy spread of the beam coming from the linear accelerator.

Because of the large field gradients in the magnets, the allowable aperture in the Collider arcs is small. This requires a very good correction of the central beam path. Accurate correction is also required because distortion of the central path causes an additional growth in beam emittance which should be minimized. For a short range magnet-to-magnet misalignment error of 0.1 mm and an error in the beam position monitor location of 0.1 mm we find that after correction, the beam-path distortions are typically $\delta x \simeq 0.5$ mm and $\delta y \simeq 0.4$ mm (rms). The associated increase in beam emittance due to beam-path errors alone is, at 50 GeV, $\delta\varepsilon_x = 0.60 \times 10^{10}$ rad m, $\delta\varepsilon_y = 0.30 \times 10^{-10}$ rad m.

3.4 Beam-Beam Effects

The maximum magnetic field within the collider bunch at the interaction point is roughly a megagauss. This large field can cause a mutual pinch of the two beams which can strongly affect the particle densities and, hence, the luminosity of the machine. For sufficiently strong fields, plasma instabilities may occur.

The effect of the beam-beam interaction can be parameterized by the dimensionless disruption parameter D.[7] For round Gaussian beams, D is given by

$$D = \frac{N r_e \sigma_z}{\gamma \sigma_r^2} \tag{7}$$

where N is the number of particles in the bunch, r_e is the classical electron radius, σ_z is the longitudinal bunch rms length, γ is the energy in rest mass units, and σ_z is the radial bunch rms width. For small values of D, the effect on a particle traveling near the axis is equivalent to that of a thin lens with a focal length f given by $D = \sigma_z/f$. As D becomes large, the beam is anything but a thin lens and strong disruptions of the beams can occur. In the language familiar from storage ring terminology, D can be written in terms of the linear tune shift $\Delta\nu$ and the interaction region beta-function as

$$D = 4\pi \Delta\nu \sigma_z/\beta^* \tag{8}$$

D can be of order one for the very small β^* interaction regions which some storage ring groups are planning to test.

For those familiar with plasma instabilities, the disruption parameter can be written in terms of the plasma frequency as

$$D = (\pi/2)^{1/2} W_p^2 \sigma_z^2/C^2 \tag{9}$$

The number of plasma oscillations (n) a test charge would make in a beam is approximately given by

$$D \approx 10\ n^2 \tag{10}$$

Figure 4 shows the results of a three dimensional cloud-in-cell computer simulation of the interaction of two beams at D = 10. There is a mutual interaction which reduces the cross sectional area of both beams during the interaction and thus enhances the luminosity. This luminosity enhancement factor is shown as a function of D in Fig. 5.

Fawley and Lee[8] at Lawrence Livermore Laboratory have modified a plasma program to look at these effects and at the onset of the kink instability. Their work confirms the work of Hollebeek and indicates that plasma instabilities should not occur for D less than roughly 30.

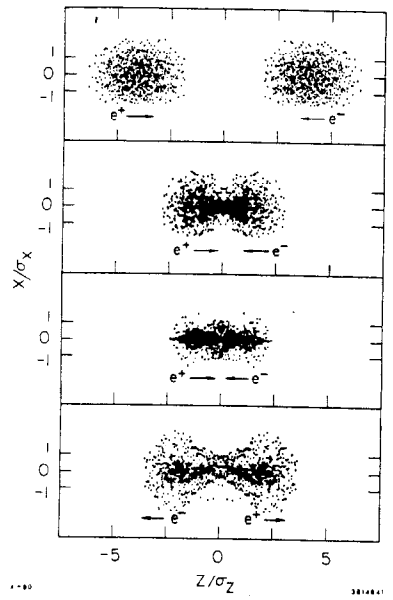

Fig. 4--Side view of the collision of oppositely charged beams, showing the pinch effect for Gaussian profiles and a disruption factor D = 14.4.

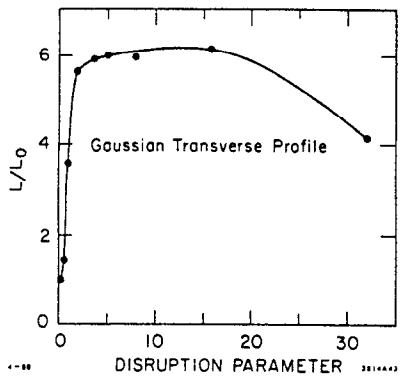

Fig. 5--The ratio of the actual luminosity, including beam-beam pinch, to the unperturbed luminosity as a function of the disruption factor for two beams with Gaussian transverse and longitudinal profiles.

3.5 Luminosity

3.5.1 Initial Design Luminosity

The luminosity of the SLC is given by

$$\mathscr{L} = \frac{N^2 f \gamma}{4\pi\beta^* \ (\epsilon_{nx} \ \epsilon_{ny})^{1/2}}$$

where f is the accelerator repetition rate (180 Hz) and ϵ_{nx} and ϵ_{ny} are respectively the horizontal and vertical invariant emittances of the bunches ($\sigma_x \ \sigma_x' \gamma$) at the collision point. The final emittance of each bunch is determined by its emittance as it leaves the damping ring, which is increased by the effects of transverse wake-field in the linac, and by quantum fluctuations in the synchrotron radiation emitted in the Collider arcs as affected by the orbit distortions in the Collider arcs and also by the bending required for chromatic corrections in the final focusing system.

The damping rings operate at a fixed energy and thus always launch a bunch with the same emittance, independent of the final linear accelerator energy.

The emittance growth caused by the transverse wake-field is a complex phenomenon for this effect depends on the linac alignment tolerances, on the charge per bunch, and on the accelerating gradient in the linac. For our alignment tolerance the emittance growth from the transverse wake effects is a constant if

$$\frac{N \ \ln(E_f/E_o)}{G} = \text{Constant}$$

where G is the accelerating gradient, E_f is the final energy, and E_o is the damping ring energy. In determining the Collider luminosity as a function of energy, we include a fixed invariant emittance growth and constrain N as a function of E_f by the above equation.

The contribution to the emittance from quantum fluctuations in the synchrotron radiation emitted in the Collider arcs and in the final focus

system are each proportional to the fifth power of the final energy. The individual contributions to the emittance are given below.

Invariant Emittance (m-rad)

Source	ϵ_{nx}	ϵ_{ny}
Damping ring	2×10^{-5}	2×10^{-5}
Linac transverse wake	0.34×10^{-5}	0.34×10^{-5}
Collider arc	$0.94 \times 10^{-5} \left(\frac{E}{50}\right)^5$	--
Orbit distortion in arcs	$0.58 \times 10^{-5} \left(\frac{E}{50}\right)^5$	$0.26 \times 10^{-5} \left(\frac{E}{50}\right)^5$
Final focus	$0.28 \times 10^{-5} \left(\frac{E}{50}\right)^5$	

The luminosity as a function of energy is shown in Fig. 6 for a β^* of 1 cm. At low energy, the quantum effects are negligible and the luminosity increases slightly faster than linearly from the increase in γ and from the increase in N allowed by the transverse wake effect. The effects of the synchrotron radiation have become significant at 100 GeV and if we were to increase the linac energy, these effects would make the luminosity peak at 120 GeV and then decrease.

3.5.2 Possibilities for Luminosity Improvement

The luminosity shown in Fig. 6 is different in character from the limiting luminosity which can be attained in storage rings. In storage rings the limit is believed to be fundamental (the limiting tune shift effect), while in the Collider the limit is imposed by various technical factors. There are significant possibilities for improvement, some of which are discussed below.

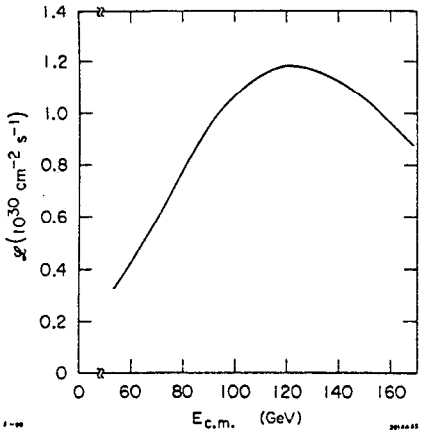

Fig. 6--Initial design luminosity vs center-of-mass energy.

One possibility, which is evolutionary, is to attain more precise control of the trajectory in the linac. This would allow an increase in the number of particles per bunch before exciting serious emittance growth from the transverse wake-field. A reduction of a factor of 2 in the trajectory errors allows an increase of approximately 2 in the luminosity.

Another improvement would arise from a decrease in the β function at the collision point from 1 cm to ½ cm which would increase

the luminosity by a factor of 2. A modified final focusing system, which has a lower value of β^*, is under design.

The beam-beam pinch effect will also increase the luminosity. At a β^* of 1 cm the disruption parameter D is approximately 0.4 and the pinch effect increases the luminosity by approximately 30% (not included in Fig. 6). However, with a β^* of ½ cm, D is increased to 0.8 which greatly strengthens the pinch and gives a luminosity enhancement of a factor of 3 over that obtained with the reduced β^* alone.

From a combination of all these effects we believe that the ultimate luminosity of the SLC may be about 10^{31}.

4. TECHNICAL COMPONENTS[9]

4.1 Linac Improvements

4.1.1 Energy

The energy of the linac will be increased to about 50 GeV by installing the second stage of the SLED rf pulse compression system (SLED II).[3] The already operational SLED I system gives an effective peak power of about twice that of the non-SLED mode. SLED II gives a further increase by lengthening the SLAC klystron pulse from 2.5 to 5 μs. This gives the storage cavities a longer time to charge up, making the effective power increase a factor of 3.2.

The SLED II system has been tested on several klystrons. We are now converting 8 klystron stations on the linac to the SLED II mode and will shortly be able to begin more extensive tests.

The maximum energy of SLED II with the available complement of klystrons and accelerator sections is 51.6 GeV. In practice, the energy will be lower because the bunches will have to ride ahead of the crest of the rf wave to compensate for the effects of the longitudinal wake fields. With our intensity of 5×10^{10} particles per bunch most of the charge will be contained within 400 MeV or a $\Delta E/E$ of 0.8% (see Fig. 3).

4.1.2 Beam-Guidance System

The design value of the beam emittance at the end of the SLAC linac is 3×10^{-10} radian-meters at 50 GeV. If there were no risk of emittance growth in the linac, the present linac focusing system would probably be adequate. However, the focusing system for the SLC has to be strengthened considerably to control the transverse wake field effects. Steering and position detection will be required at each quadrupole to control the effects of all the transverse fields including the wake fields produced by the bunches themselves, the stray DC fields produced by quadrupole misalignments which deflect the electrons and positrons in opposite directions, and the rf fields from accelerator misalignments and coupler effects which deflect the electrons and positrons in the same direction.

The lattice that has been chosen is a FODO array with 12.5 meter quadrupole spacing and with an extra quadrupole singlet at the end of every sector where there is a 3-m drift section, i.e., a total of 9 quadrupoles per sector. Each of the 270 quadrupoles will carry four extra trim-windings for vertical and horizontal steering, and each will contain (within the vacuum chamber) an x-y strip-line position monitor. The maximum integrated gradient-length that is practical in the available space is about 107 kilogauss. It is possible to maintain a 90° betatron phase advance per cell up to 25 GeV then tapering down to 42° per cell at 50 GeV.

In parallel with these efforts, a plan is being developed to make full use of the capabilities of the laser alignment system of the accelerator. By design, this system is believed to be capable of ~25 μm alignment reproducibility, with absolute rms errors of about 100 μm. In recent years it has rarely been used to these tolerances, which have simply not been needed to satisfy accelerator operation (alignment to 250 μm has generally been sufficient).

4.2 The Collider Lattice

4.2.1 General

It is the function of the magnet lattice in the Collider arcs to bend the high-energy e^+ and e^- beams from the SLAC accelerator in such a manner that they will collide head-on with as little dilution of phase space and loss of energy as possible. Quantum effects in the synchrotron-radiation discussed in section 3.3 speak for a lattice of large radius containing many short high-gradient magnets of small aperture. In the adopted design ρ is approximately a site-limited 300 meters, the maximum guide field B_o is 8 kG, and the maximum gradient is g = 10 kG/cm (70 GeV operation). The tune of an equivalent circular machine would be around $\nu \simeq 100$, with an average $\overline{\beta} \simeq 3$ m. For phase advances between 90° and 130° per FD cell, the magnets are typically around 2 meters in length.

4.2.2 Magnet Profile

The first published article on strong focusing[10] contains the basic design of a magnet having the required characteristics. Our magnet is modeled on it and has a cross-section shown in Fig. 7. The distance between the position of the equilibrium orbit and the neutral pole is $K = B_o/g = 8$ kG/10 kG/cm = 0.8 cm. Studies[11] with the program POISSON show that a good field region of ±5 mm is obtainable. Such a region is adequate to contain the miniscule beam size $\sigma_x \simeq \sigma_y \simeq 0.03$ mm, with additional room for initial orbit distortions of several millimeters. The pole profile will be shaped to produce a mild sextupole term to cancel chromatic effects in the arcs.

An analysis of capital construction costs in relation to operating power costs indicates the use of aluminum as a conductor material and a generous

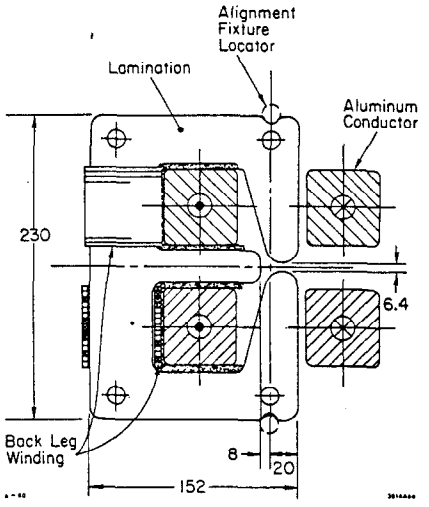

Fig. 7--Cross section of the SLC arc magnets. Dimensions are in millimeters.

Table 3

SPC main ring bend magnet parameters at 50 GeV

Magnet designation		6AG2400
Number of magnets		635
Field @ 50 GeV	(kG)	5.7
Field integral @ 50 GeV	(kGm)	13.68
Gap height	(mm)	6.4
Width of good field	(mm)	10
Core length	(mm)	2394
Core weight	(lbs)	1034
Lamination width	(mm)	155
Lamination height	(mm)	230
Amp-turns/pole		3830
Turns/pole		1
Conductor area	(mm^2)	2733
Cooling hole diameter	(mm)	17.8
Power	(kW)	1.66
Current density	(A/mm^2)	1.4
Coil weight	(lbs)	158

coil window. Some parameters of the arc magnets, including the reverse-bend transport system magnets, which are of indentical design, are shown in Table 3.

4.2.3 Construction

A circumference-filling factor of about 95% is made possible by threading 4 magnet cores on common coil conductors and a "refrigeration tubing" vacuum chamber to form modules. Only a few centimeters remain between core blocks for miniature position-monitor stations. To facilitate installation by minimizing work in the narrow tunnel, it is planned that each 10-meter-long module be completely assembled, to some extent aligned, and contain the complement of services, cabling, pumps, instrumentation, etc., necessary for operation. All that should be required in the tunnel is to roll in prefabriacted modules, mount the girder, interconnect the busses, cabling harness and vacuum, and perform final alignment.

The Collider arc tunnels, for site-related reasons, are not in a horizontal plane. To simplify the resulting survey problems, each arc is segmented into three planes, one down, one level, and one up. The grades are less than 10%. The connection between planes will be accomplished by turning the standard arc magnet through 90° on selected modules. If the phase shift per vertical bend is appropriately chosen, the problem of matching the vertical η function is eliminated.

Four separate solid extruded aluminum water-cooled conductors form the coil. The water channel is designed for low velocity flow (approximately 2-3 ft/sec) to minimize vibration. All magnets are run in series by a common power supply regulated to 0.01%, which is supplemented by a low-power servoamplifier to improve regulation by another factor of 2.

Each magnet will have two 15-turn back-leg windings. When these windings are connected to aid each other, they produce a 4% $\Delta B/B$ horizontal trim at 50 GeV, or three times the variation in B_o expected to be caused by magnet-to-magnet alignment. When connected to buck, vertical steering results. Since over 1200 magnets are involved, new concepts in trim power-supply control are called for. Computer-controlled D-to-A packages delivering 10 amps at 5 volts are envisioned.

4.2.4 Ground Motion

Since the invention of strong focusing, it has been recognized that severe tolerances are placed on the position of magnetic elements. We have assumed above that a steady-state correction system will be effective in steering the beams around the transport arcs at the fractional millimeter level. In order to collide beams successfully at the interaction point at the micron level, however, a supplemental dynamic position feedback system is also required. This system derives its positional information from previous pulses. Since the Collider operates at 180 pps, the upper limit to the bandwidth of this system is 30 Hz.[12] One must examine, therefore, whether disturbances occur above this frequency of sufficient amplitude to cause troubles. This has been done. Ground motion in the PEP tunnel and near the boundaries of the Collider site has been measured[13] in the frequency range of 0.1 to 100 Hz over a period of several days. These studies lead to the following conclusions.

1) Ground motions arising from natural causes such as earth tides, earthquakes, microseismic noise due to storm action, etc. have either steady-state amplitudes above 2 Hz that are negligible compared to the 0.2 micron rms relative magnet stability required, or else they occur very infrequently. Below 2 Hz, the wavelengths of the disturbances are larger than the Collider site and, therefore, not of importance in relative magnet motion. In addition, the feedback system can cope with them.

2) Careful design of buildings and structures is indicated to suppress the effects of steady-state noise generated by pumps, ventilation fans, transformers, compressors, and the like.

3) Of the other cultural (i.e., manmade) disturbances, the most commonly found were peak disturbances (amplitudes in the few-micron range, lasting seconds) associated with traffic. Fortunately, the worst daytime event rates are a few per hour, low enough to be acceptable. During the night the frequency is typically much less.

4.3 Final Focusing System

4.3.1 General

The purpose of the final focusing system is to demagnify the beam size from the Collider arcs to a size suitable for beam collisions, and also to correct for the chromatic depth-of-focus caused by the finite momentum spread in the beam. This is accomplished in a system 114-meters long, using practical magnet strengths, with four half-wave magnetic-optical transformers. The overall system is shown in Fig. 8. The first two transformers match the

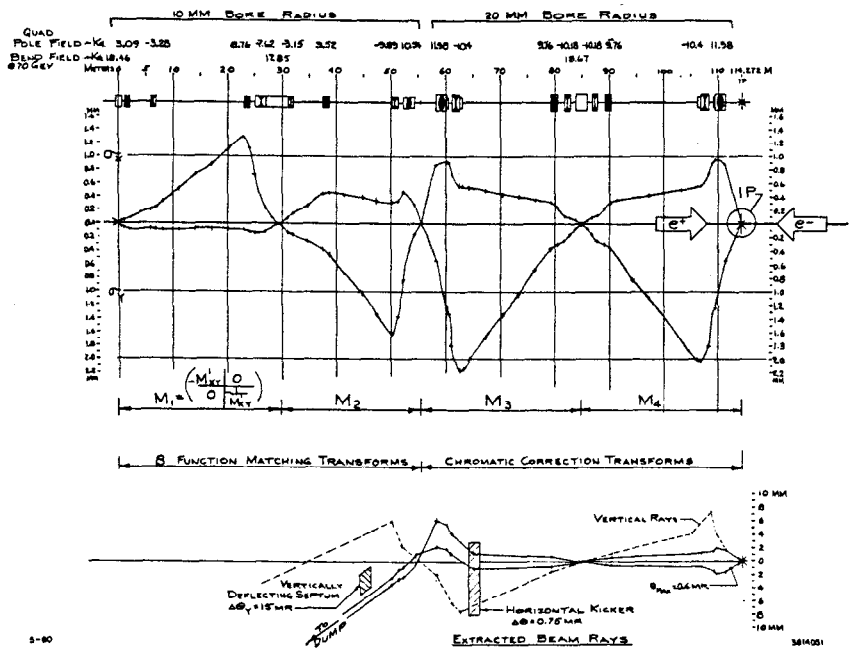

Fig. 8--Schematic representation of the final focusing system.

monoenergetic beta functions in the arc lattice to a interaction-point (ip) beta function of 1 cm. The last two transformers are used to make the chromatic corrections. They are identical but placed in mirror symmetry. Contained within each of the last two transformers are two sextupoles, one for the x plane and one for the y plane, which correct the chromatic aberrations causing the depth-of-focus problem. Dipoles are inserted (one at the end of the arc lattice, one between transformers 1 and 2, and one between transformers 3 and 4) so as to introduce an appropriate dispersion into the system to make the chromatic correction possible. The dipole strengths are chosen so as to minimize the higher order optical aberrations at the interaction point. The beta function at the position of the dipoles is chosen so as to restrict the emittance growth caused by synchrotron radiation to an acceptable value.

4.3.2 Focal Spot Size

Figure 9 is a scatter plot of 3000 rays traced through the system using a special program which takes into account higher order geometric and chromatic terms to all orders. The input transverse phase spaces assumed are Gaussian with $\sigma_x = \sigma_y = 0.0367$ mm, $\sigma'_x = \sigma'_y = 0.00825$ mr. Energy spread is a flat distribution with $\Delta E/E = \pm 0.5\%$.

The output distributions will not be pure Gaussian in form due to the effects of the high-order terms. For this reason circles containing fractions of the beam's population are shown. The projected Δx, Δy distributions show "equivalent" rms widths of $\sigma_x \simeq \sigma_y \simeq 2.1$ microns, $\sigma'_x \simeq \sigma'_y \simeq 0.14$ mr.

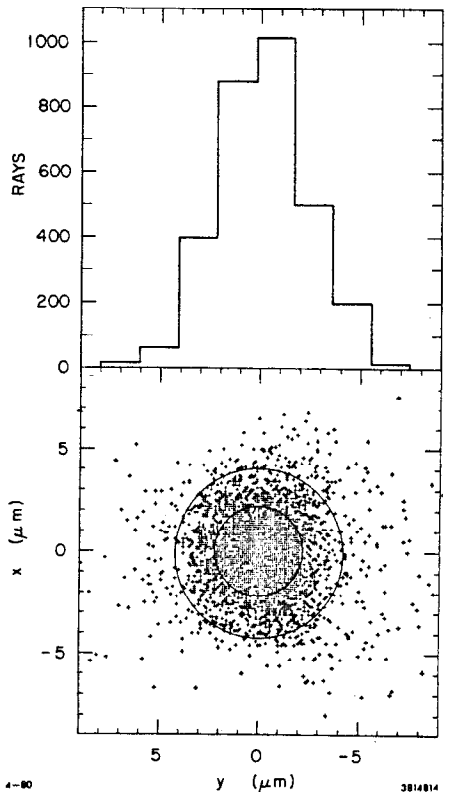

Fig. 9--A scatter plot of 3000 rays traced through the final focusing system. The inner and outer circles enclose, respectively, 50% and 90% of the charge.

4.3.3 Aperture Requirements

As can be seen in Fig. 8, the aperture of the magnets in this system need not be very large for the incoming beam. However, after the beams strike each other, the "disruption" of the collision will magnify the output angles. In order to ensure that background is not created by the spent particles before they are extracted and disposed of, the transport system's aperture has been chosen to be 4 cm. With such an aperture, pole-tip field strengths remain below 12 kG in the larger quadrupoles at 70 GeV. The design of these high-gradient, small-aperture lenses, which traditionally run with high current densities, is being carefully optimized with power consumption in mind.

4.4 Positron Source

The positron source for the Collider will be located at the 2/3 point of the linac where the electron beam will have an energy of 33 GeV. Thus, the new source must have an efficiency of 3% per GeV of incident electron energy for the production of positrons into the 6 dimensional phase acceptance of the damping ring. The present SLAC positron source has an efficiency of 1½% per GeV. The increased yield will be attained by increasing the target Z and increasing the transverse acceptance of the focusing system.

The focusing system is designed to accept an e^+ energy at the target of from 2-20 MeV with a transverse emittance of 5 MeV-mm. Some of the parameters of the new source are given in Table 4.

Table 4

Positron source specifications

A. EXTRACTION SYSTEM

Beam:		
	Electron energy	33 GeV
	Pulse energy	194 Joules
	Power	35 kW
	Intensity	3.7×10^{10} electrons/pulse
	Pulse rate	180 Hz
	Size	0.4 to 1.0 mm (standard deviation)

B. TARGET SYSTEM

Material	74%W - 26%Re
Energy deposition	39 Joules/pulse
Pulse temperature rise	200-480°C
Maximum compressive stress	60,000-140,000 psi
Length	6 radiation lengths = 21 mm
Power deposition	7 kW
Maximum pulse temp.	800-1100°C
Steady-state temp.	600°C

C. COLLECTION SYSTEM

Beam:		
	Energy range at target	2-20 MeV
	Emittance	2 mm × 2.5 MeV = 5 MeV-mm
	Yield	$e^+/e^-_{in} = 4.8$

Initial Magnetic Focusing:

	Length (m)	Field Range (kG)
Pulsed tapered solenoid	0.15	100 - 15
DC tapered solenoid	0.40	15 - 5
DC uniform solenoid	6	5

4.5 Beam Damping and Compression

The purpose of the damping rings is to reduce the emittances of both e^+ and e^- beams to values suitable for the attainment of high luminosity. The e^+ emittance must be reduced by about a factor of 1000, while the e^- emittance must be reduced by about a factor of 10. This is done by using the radiation damping in two small high-field storage rings. The compressors' function is to reduce the bunch lengths of the beams emerging from the dampers ($\sigma_z \approx 1$ cm) to sufficiently small values ($\sigma_z \approx 1$ mm) so that an acceptably small energy spread (±0.5% will result after final acceleration. Such a maneuver is performed by exchanging $\Delta\phi$ with ΔE in longitudinal phase space.

4.5.1 Damping Rings

The method behind the choice of damping ring parameters is described in reference 14, where it is noted that realizable magnet strengths and the rise-times of injection and extraction kickers determine these parameters. Using a maximum field of 20 kG in the bends, the resulting parameters are listed in Table 5. The ring energy is 1.21 GeV. Two bunches circulate in each ring; hence by extracting alternate bunches the effective cooling period ($T_c = 4\tau$) is made twice the linac interpulse period of 1/180 sec. In order

Table 5

Damping ring parameters

Energy	1.21 GeV
Number of bunches	2
Circumference	34.01 m
Bending radius	2.049 m
Damping times	τ_x = 2.821 ms; τ_y = 2.959 ms; τ_z = 1.517 ms
Magnets	
Bends (40/ring):	B_o = 19.7 kG, length = 31.1 cm
Quads (48/ring):	g = 6.45 kG/cm, length = 10.2 cm
Beam stay-clear:	x = ±5 mm, y = ±6 mm
Tunes	ν_x = 7.106, ν_y = 3.125
Input phase space for positrons	
	$\varepsilon = 4.1 \times 10^{-6}$ π rad-meters at 1.21 GeV
	ΔE/E = 1%
	(phase space for electrons is much smaller)
Output phase space	
	For coupling K = 1, $\varepsilon = 2.6 \times 10^{-9}$ π radian-meters
	ΔE/E = 0.073%
Radiofrequency system	
	Revolution frequency: 8.814 MHz
	U/turn: 0.093 MeV
	RF frequency (example only): 969.57 MHz, h = 110
	RF voltage: 0.220 MV
	Current (2 bunches): 141 ma
	Synchrotron radiation power: 13.1 kW; Cavity power: 3.0 kW
	Synchrotron tune: ν_z = 0.0073
	Bunch length: σ_z = 1.0 cm
Vacuum	P less than 10^{-6} Torr
Polarization time	τ_p = 11 minutes (too long to be useful)

not to disturb the "half-damped" bunch, the sum of the rise and fall times of either injection or extraction kicker is one revolution period, or a realizable 100 nanoseconds.

Each ring has a separated-function structure. In the arcs, the magnet-filling factor is only about 50% to allow room for the coil ends of the magnets. For such a small ring the tunes ν_x = 7.106, ν_y = 3.125 are relatively high. Both positive and negative sextupole fields, necessary for the control of the head-tail instability, will be introduced at each end of the bends by pole-end shaping. The aperture is set by the phase-space of the injected beam, with allowance for orbit distortions. The energy acceptance ΔE/E is ±1%. Kickers are located in two of the four 0.4-meter straight sections, with vertically deflecting septa in the 1.2 m straight sections.

The requirements for the radiofrequency and vacuum systems are quite modest. The rf system provides 16 kW to compensate for the synchrotron

radiation and cavity losses. An average pressure of only about 10^{-6} Torr is required, since storage times are in the tens of milliseconds. This is fortunate because the small-aperture vacuum chamber will be conductance-limited and difficult to pump to a much lower pressure.

Pre-acceleration to the operating energy of 1.21 GeV is required. Thus, the rings are located between Sectors 1 and 2 of the SLAC linac, using the first linac sector as the booster. The two damping rings are stacked vertically to conserve space in the underground vault.

In order to launch the damped and phase-compressed beams back onto the linac axis with the tolerances required, one must hold the pulse-to-pulse jitter in position and angle of the extracted beam to $\Delta x_o \approx 30$ microns, $\Delta\theta_o \approx 2$ microradians. The only time-dependent magnets in this process are the extraction kickers. Assuming a kicker deflection angle of, say, 2 milliradians, this implies an amplitude stability of $\approx 0.1\%$.

4.5.2 Compressor

The scheme for bunch-length compression is described in reference 6. The object is to reduce σ_z of the bunches as they leave the damping rings from 1 cm to 1 mm. This is done by "accelerating" the particles of the bunch at 0^o central phase, thus introducing a strong correlation between position and energy, and subsequently passing the bunch through a non-isochronous transport system such that the higher energy particles travel a longer path and hence arrive at the linac entrance at almost the same time as all others.

Thirty megavolts of rf acceleration are required, a demand that can easily be met by a standard SLAC 10-ft linac section driven by a klystron. This equiment is already on hand. Transport to the linac is via a smooth 90^o arc of average radius 19 meters containing some ten bends and approximately fifteen quadrupoles. A horizontal aperture of 5 cm is enough to accommodate the maximum dispersion required. The required bending fields of 8 kG and quadrupole gradients of 1 kG/cm are modest. Emittance growth in this arc has been found to be negligible.

4.6 High Current Electron Source

The electron source for the Collider must produce two intense electron pulses for each cycle of operation: one for the actual collisions, and one to produce positrons for later collisions. Each of these electron pulses must result in 5×10^{10} electrons being captured and transported to the electron damper ring. The emittance of these pulses must be small enough to be damped to the value required for Collider operation during two betatron damping times of the damper ring.

The electrons will be generated by photoemission from semiconductor cathodes. SLAC has experience in operating such electron guns on the linac. They have been used to provide the polarized electron beam for the recent

inelastic scattering parity-violation experiments, though at much lower peak current than required here. Development work has continued since those experiments, and currently we have been able to produce cathodes which show promise of meeting the design requirements and of having a high degree of longitudinal polarization.

While it appears likely that photoemission cathodes could directly generate an electron pulse containing 5×10^{10} electrons and lasting only 100 to 150 psec, computer simulations indicate that the space-charge phenomena associated with such a bunch are so severe that it may not be possible to bunch and capture all of this charge into a single S-band bunch in the linac. Since these problems decrease significantly as the electron bunch becomes longer, we have decided to employ a subharmonic buncher between the electron gun and the S-band linac. In this scheme, initial bunching will be accomplished at the 16th subharmonic (178 MHz) of the linac rf frequency. This will allow the electron pulse from the gun to be up to 1.5 nsec long, thus eliminating most of the ill effects associated with the higher charge density of the 100 psec bunch. The subharmonic buncher itself will consist of a single cavity and a drift section. Subharmonic bunching has been used to achieve single bunches containing more than 5×10^{10} electrons in an L-band linac at Argonne.

The bunch from the subharmonic bunching section will enter a standard SLAC injector section, exactly like that used presently on the linac. At the output of this section, the beam will be fully bunched and will have an energy of about 50 MeV. Solenoidal focusing will be used along the entire length of the subharmonic buncher and the injector section.

The laser gun can produce longitudinally polarized electrons. To prevent depolarization in the damping ring, the polarization vector must be rotated into the vertical direction before injection into the damping ring, and rotated back to longitudinal after extraction from the ring. At 1.2 GeV these manipulations can easily be done by a combination of bending magnets and solenoids. The longitudinal polarization at the collision point that might be expected is shown in Fig. 10 as a function of center-of-mass energy.

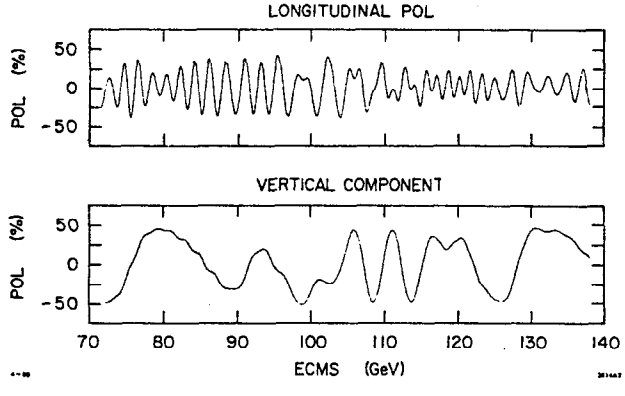

Fig. 10--A model calculation of spin projections in the interaction region as a function of center-of-mass energy, for 50% polarization leaving the linac. The g-2 precession of the electron spin results in rapid oscillations of the longitudinal component and rather slower oscillations of the vertical component from a beam-transport system that approximates the north arc of the Collider ring.

5. CONCLUSION

We are all familiar with the "Livingston plot" which shows the increase of accelerator energy with time. Historically, a given technique reaches its limit and a new technique takes over with the result that the energy of fixed target accelerators has been increasing by a factor of 10 every 6 years -- equivalent to a factor of 10 in center-of-mass energy every 12 years. This historical trend is also true for electron colliding beam machines as is shown in Fig. 11 where the energy of the leading electron colliders is plotted vs time. The slope of this curve is a factor of 10 every 10 years; equal to within the errors to that for the conventional machines.

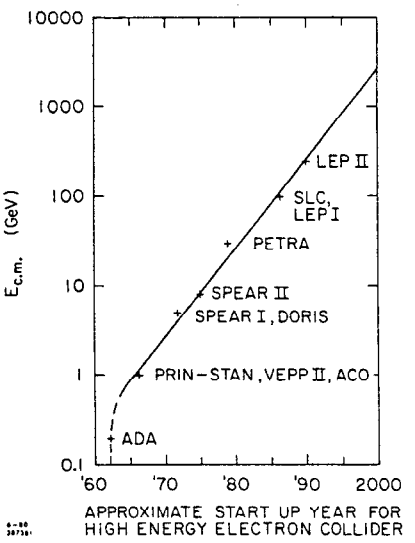

Fig. 11--Time dependence of the energy of electron colliders. Only the highest energy new machines are indicated.

The slope of the curve has two sources. One is the time required by the accelerator community to understand the technical problems at a given energy and to be prepared to make the next step. The other is the time required by the experimental and theoretical communities to obtain the data at a given energy, to understand its implications, and to formulate the appropriate questions to be addressed by the next machines. Of course, the development is not so orderly and rational as I have indicated, but I think it does basically proceed as I have outlined.

The electron storage ring technique is reaching its limits because of its rapid increase of cost with energy. Linear Colliders will take over from storage rings, for the needs of physics for the answer to questions which can only be addressed at higher energies will require new machines beyond LEP.

Much technical development will be required before a very high energy Linear Collider can be economically constructed. We at SLAC believe that the SLC is a proper first step in the development of the new technique for it gives both the chance to do important experimental physics and the chance to understand the new questions of the beam dynamics of the intense bunches of particles which will be required for any Linear Collider. The SLC is thus novel, timely, and can be a productive physics tool. We hope we will have the chance to build it.

REFERENCES

1) A good summary of the history of Linear Colliders with references is given in U. Amaldi, Proceedings of the IXth International Symposium on Lepton and Photon Interactions, 314, Fermilab (1979).

2) B. Richter, Nucl. Inst. & Methods, 47, 136 (1976).

3) G.H. Loew, Proceedings of the Xth International Conference on High Energy Accelerators, Serpukov, USSR (1977).

4) A.W. Chao, B. Richter, C. Y. Yao, contribution to this conference.

5) M. Sands, Physics with Intersecting Storage Rings, Academic Press, New York (1971).

6) R.D. Helm and H. Wiedemann, PEP Note 303, SLAC (1979).

7) R. Hollebeek, SLAC-PUB-2535 (1980), submitted to Nuc. Inst. & Methods.

8) W.M. Fawley and E. P. Lee, Lawrence Livermore Laboratory Report UCID-18584 (1980).

9) A more detailed technical description of the Collider is given in SLAC Linear Collider Conceptual Design Report, SLAC Report 229, 1980.

10) E.D. Courant, M.S. Livingston, H. Snyder, Phys. Rev. 88, 1190 (1952).

11) G.E. Fischer, SLAC Report AATF/79/5 (1979).

12) R. Stiening, SLAC Report CN-14 (1980).

13) G.E. Fischer, SLAC Report AATF/80/18 (1980).

14) H. Wiedemann, SLAC Report AATF/79/8 (1979).